

Chapter 3

Experimental setup

experiment is set up and

This chapter presents briefly the structure and the characteristics of the Mainz microtron accelerator (MAMI), where the transverse asymmetry is measured, and the experimental setup used. Particular attention is given in the description of the beam monitors, that are quite specific for the standard of particle accelerators. Following an overview of MAMI and the acceleration stages, the experimental hall and the specific electronics devices to acquire and process the data are presented.

used

3.1 Overview of the Experiment

target is thick

To measure the Beam-Normal single spin asymmetry, a polarized beam of 570 MeV will be sent against a 10 mm width of ^{12}C target. The detectors consist of two fused-silica bars coupled to 3 (detector B) and 8 (detector A) PMTs, which collect the Cherenkov light emitted when an electron pass through the fused-silica. The detector are placed inside the two spectrometer of the A1 hall, whose standard of which are not used in this experiment due to the high luminosity of the beam ($20 \mu\text{A}$) that is above their limits of operation. The asymmetry the between two orientations of the beam is the goal. The PMT signals are collected and digitalized by the NINO board, after a threshold selection, and sent to the A1 control room computer, where the DAQ program collect the data together with all the data coming from the Beam monitors, producing binary files, which are later analyzed by the analysis program, which is significant part of the work done in the framework of the thesis. The data collected are divided in Events made by 4 sub-events in sequence. Each event correspond to a temporal window of ≈ 80 ms, where each sub-event is 20 ms long. Here it's important to clarify that, unlike the majority of experiments in high energy physics, an event is made by all the electrons interacting with the detectors during the time interval of the event, and we will refer to this hereafter unless otherwise stated. The division into sub-events reflects the polarization sequence of the beam. The PMTs counts and the beam monitor values are saved for each sub-event, along with the time length of the event (measured by the clock cycles by the NINO electronic board), and other values which are required to process beam monitor data.

The general structure of the event is the following:

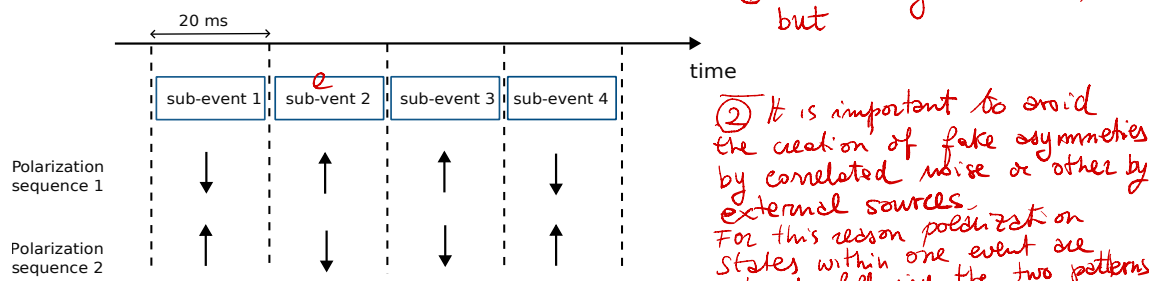


Figure 3.1: General structure of the event. The gate-length of each event is synchronized with the power grid frequency, to reduce possible effects of 50 Hz noise.

The particular choice of 20 ms for the sub-event is due to avoid possible, not desired effects generated by the power grid frequency (not 50 Hz). The gate-length of each sub-events is synchronized with the period of the power grid frequency, to ensure that electronic noise does not produce effects between nearby sub-events. For each event we have a single measure of A_n , defined as the asymmetry between the \uparrow and \downarrow sub-events. At

moment

questo non è chiaro,

Event \rightarrow event \rightarrow parte in inizio
di fine
azione

the beginning of an ~~event~~ one of the two polarity pattern is selected using a De Bruijn sequence. A De Bruijn sequence of order n is defined as a cyclic sequence where every sub-sequence of length n appear only once. We have two different polarization pattern, the ones shown in the figure, that can be represented as 1 and 0. For this experiment, the De Bruijn sequence is of order $n = 6$ bits; this correspond to all the possible sequences of 1 and 0 with a length equal to 6, which are 64 different sub-sequence. It's possible to demonstrate that ~~exist~~
~~exactly~~ N_{bruijn} sequences ~~is~~ \downarrow

De Bruijn

$$N_{bruijn} = \frac{(k!)^{k^{n-1}}}{k^n}$$

If we substitute in the formula above $k = 2$ and $n = 6$, we have a total of $\simeq 67 \cdot 10^6$ different sequences. The seed of the De Bruijn sequence is generated with a pseudo random number generator, and the sequence is used to select between $\uparrow, \downarrow, \downarrow, \uparrow$ and $\downarrow, \uparrow, \uparrow, \downarrow$. At this point it could be objected why so much care is taken in choosing randomly the two sequences. At a first glance is certainly easier to select one of the two polarization pattern and reproduce it for every sub-event. However, this does not protect from systematic effects that arise from electronic or beam noise with frequencies similar to the frequency of the ~~polarity~~ pattern. An electronic noise, with a frequency roughly 10 Hz could in principle increase the rates for one polarizations state and decrease the other. The adopted solution to reduce possible effect is to randomize the pattern selection. In the end, there is another reason why a ~~DeB~~ sequence is useful. During each polarization flip, we observe a short, transient reduction of the beam current. This reduction in the beam intensity has more influence on patterns where there are more inversion of the ~~polarity~~ respect to the other. With a ~~DeB~~ sequence we ~~assure~~ ensure that we have an identical number of pairs of patterns, meaning that:

- 25% : $\uparrow, \downarrow, \downarrow, \uparrow ; \uparrow, \downarrow, \downarrow, \uparrow$
- 25% : $\downarrow, \uparrow, \uparrow, \downarrow ; \downarrow, \uparrow, \uparrow, \downarrow$
- 25% : $\downarrow, \uparrow, \uparrow, \downarrow ; \uparrow, \downarrow, \downarrow, \uparrow$
- 25% : $\uparrow, \downarrow, \downarrow, \uparrow ; \downarrow, \uparrow, \uparrow, \downarrow$

non è polarità, è polarizzazione!

In the top rows we have 4 inversions, while in the two lower rows we have 5 inversions. Later we will describes the other details of the experiment; in the next sections we will present briefly MAMI accelerator, where the experiment is performed.

3.2 Mami

MAMI is the electron accelerator located in Mainz, which provides a continuous wave, high intensity, polarized beam for nuclear physics experiments with ~~fixed-target~~. The concept of the Mainz microtron accelerator is born in the early 1970s, when the researchers of the nuclear physics institute were investigating the possibility of generalizing the concept of the racetrack microtron (RTM), that consists in a linear accelerator (linac) and two deflection magnets (180° magnet, see the figure). The particle recirculate, due to the deflection magnets, several time in the linac, and each time they gain energy. The goal of the collaboration which develop MAMI was to produce a continuous beam, with energies above 1 GeV and beam intensities up to 100 μA for ~~high efficiency in fixed-target experiments.~~ (~~grande efficienza~~) \rightarrow ~~nuovo~~

A racetrack microtron, as the one shown in the figure, is characterized by the energy gain per-cycle δE given by the high-frequency electromagnetic field (HF). The energy gain is:

$$\delta E = eU_{Linac} \cdot \cos(\phi)$$

non mi torna tanto: ma
c'è una certa soluz nel
LINAC?

U_{Linac} is the maximum voltage of the linac, and ϕ is the phase of the beam relative to the maximum of HF. Because the particle are accelerated by the linac, the beam consist in individual packets (bunches) whose rate correspond to the ~~frequency~~ of HF. In order for the electrons to be accelerated for each recirculation step, they must arrive at the beginning of the linac with the correct phase ϕ . For this it is important that the flight-time per cycle must be an integer ~~or a~~ multiple of the HF period.

Therefore

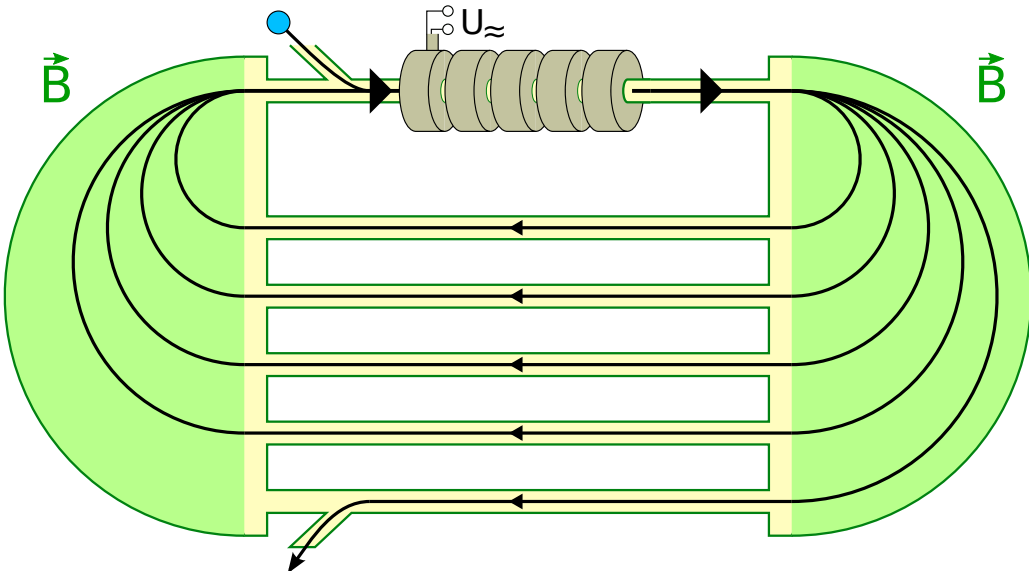


Figure 3.2: Racetrack Microtron. The particles are sent to the linac, and the two deflection magnets make the particles recirculate, until the momenta exceed the capability of the magnetic field.

Dici all'inizio che il limite pratico delle frequenze sono ~ GHz

$$f = \frac{1}{2\pi} \cdot \frac{q}{\gamma m_0} \cdot B$$

*queste non le sognhi!
le flight time contiene anche una parte fisso (3.1)
delle sezioni diverse*

From this overview two conclusion can be drawn:

- To accelerate slow electrons, with $\gamma = (1, 10)$, a magnetic field of 0.1 T is used, in order to work with frequencies of (2 GHz, 2 GHz), that are easy to control. However with higher energies the bending radii is higher, with a small magnetic field.
- For high energy electrons $\gamma > 10$, to reduce the size of the deflection magnets, it is useful to increase the ~~Magnetic~~ field up to 1 T or more. ~~This let to accelerate the electrons~~ using the same technology for $f \simeq \text{GHz}$.

These conclusions justify the structure of MAMI: a cascade of microtrons to reach each time higher energies with the same acceleration frequency at each stage. MAMI is composed by a sequence of 4 different microtrons, ~~reaching~~ to achieve energies of 1.6 GeV. The first stage, shown in figure 3.6, is composed by two small microtrons. The first microtron RTM1 accelerates the particle to 14 MeV in 18 revolutions. The electrons are then sent to the second microtron that can accelerate the particle up to 180 MeV. After passing the first stage, the beam is sent to the RTM3 (race track microtron 3), a large microtron with an end point energy of 855 MeV. These 3 microtrons forms MAMI-B, which started operation in 1990-91. A fourth stage, MAMI-C, was built and started operation in 2007. This fourth stage is made by 4 bending magnets, with a bending angle of 90°, and it is designed to achieve energies of 1.6 GeV. The design is different from the other race-track microtrons, and will not be explained, as it is not necessary for the experiment to reach such high energies.

The operation principles of a microtron are simple to be described. First we consider the gyro-radius for relativistic electrons, that is:

of energy E

$$r = \frac{E\beta}{qcB} \quad (3.2)$$

To have a coherent conditions, we must have that the flight-time $\tau = \frac{\lambda}{c}$ of the first recirculation must be an integer multiple of the HF, see equation 3.1. This means that:

$$\lambda = \tau c = \frac{2\pi c R}{\beta c} = \frac{2\pi E}{qB} = m\lambda_{HF}$$

*definisce $\lambda_{HF} = \frac{\lambda}{m}$
perché non ci mette la parte dritta?*

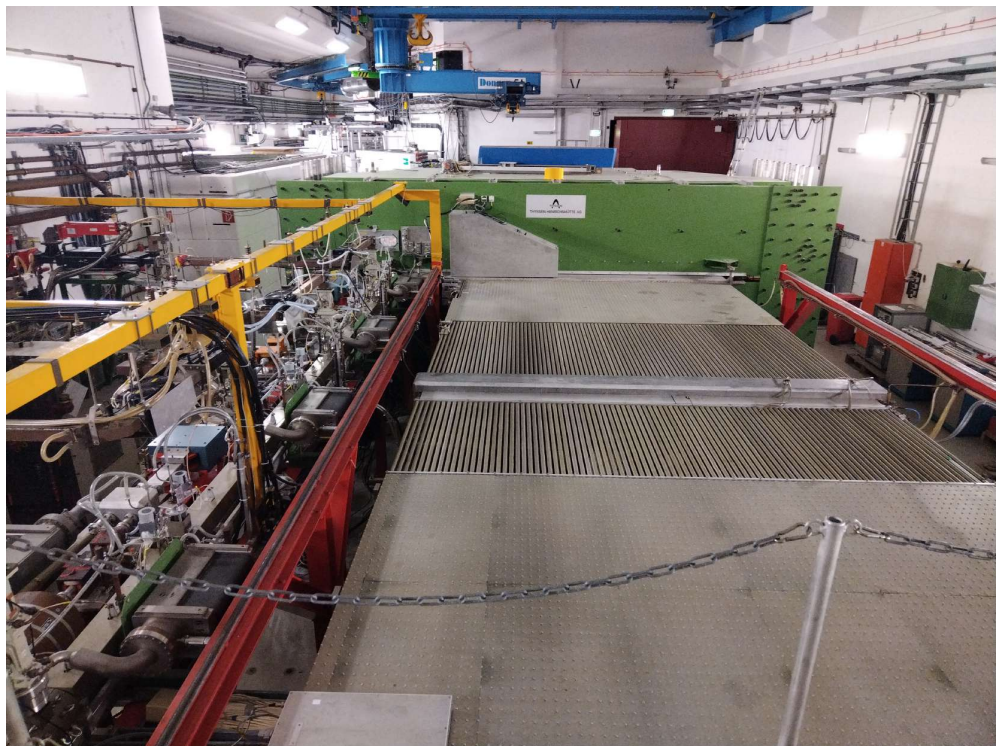


Figure 3.3: Picture of the Racetrack RTM3 in MAMI-B. The Green square at the bottom is one of the deflector magnets, the other one is below the point where the photo was taken. The linac stage is on the left. The tubes at the center of the figure are the paths that the particle cross during the recirculation. The further away from the linac the greater the energy.

For the other recirculation, we must have that the flight-time at energies $E_i = E_{n-1} + \delta E$ must be increased by an integer multiple of HF, too. This lead to the second equation:

$$\frac{2\pi\delta E}{qB} = n\lambda_{HF}$$

The minimum gain per cycle is then determined only by the strength of the magnetic field and wavelength λ_{HF} . These two equations together controls the dynamic of the race-track microtrons,

3.2.1 Polarized Beam

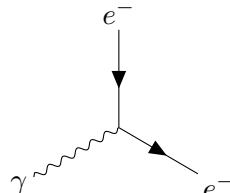
*vertical polarization
vertically polarized
by
Spin*

For the beam-normal single spin asymmetry a vertical polarized beam is necessary. At the MAMI electron accelerator is possible to produce a vertical *by* polarized beam with energy in the range 180 MeV – 855 MeV [16]. In this section the procedure to orient the *beam* vertically is presented, following an explanation of how the degree of polarization is measured.

The electron source used at MAMI is made by a strained GaAs/GaAsP super-lattice photo-cathode illuminated by circularly polarized light. To alternate the sign of the light polarization, a fast Pockels cell (||) is installed in the optical system of the electron source. The Pockels cell is a wave plate controlled by the electric field, that changes the helicity of the photons impinging on the electrons. A Pockels cell exploits the Pockels effect, that affects crystal with particular characteristics (lack of inversion symmetry). For this type of materials the refractive index is linearly dependent on the applied electric field. By controlling the refractive index with the electric field, the polarization state of the incident light beam is altered. Once an photons imping on an electron, the extracted electron carries the same helicity of the incoming photon *because*

their

of angular momentum conservation :



$$(Jz)_\gamma = \pm 1 \quad (Jz)_{e^-} = \mp \frac{1}{2} \rightarrow \pm \frac{1}{2} \quad (3.3)$$

alternate

With the fast change of the Pockels cell it is possible to alternately revert the sign of the polarization. By the insertion of a $\lambda/2$ plate between the laser system and the photo-cathode the global polarization orientation of the electron beam can be reversed. This is particularly useful because this directly changes the sign of the physical asymmetry measured by the detectors, and allows to identify systematic errors. This is useful done for longer beam time, where two sets of data are taken, reversing the orientation of the $\lambda/2$ wave plate. By comparing the results for the two sets of data, the influence of the optical system on the asymmetry measurement is estimated and can be corrected in the final result of the asymmetry. During the beam time of interest for this thesis, the $\lambda/2$ wave plate orientation was fixed. During previous beam time ([8]). The beam polarization achieved with this source is roughly $P = 80\%$, so the measured asymmetry are:

??

$$A_{measured} = P \cdot A_n$$

The polarizations of the electrons just extracted from the source is still longitudinal. The magnetic field is needed in order to rotate \vec{P} from longitudinal polarization to transverse. For this purpose two devices are used: the Wien filter and a double solenoid located in the injection beam line, close to the the optical source *bird's eye view* *no bold*, *shown Fig 3.4.*

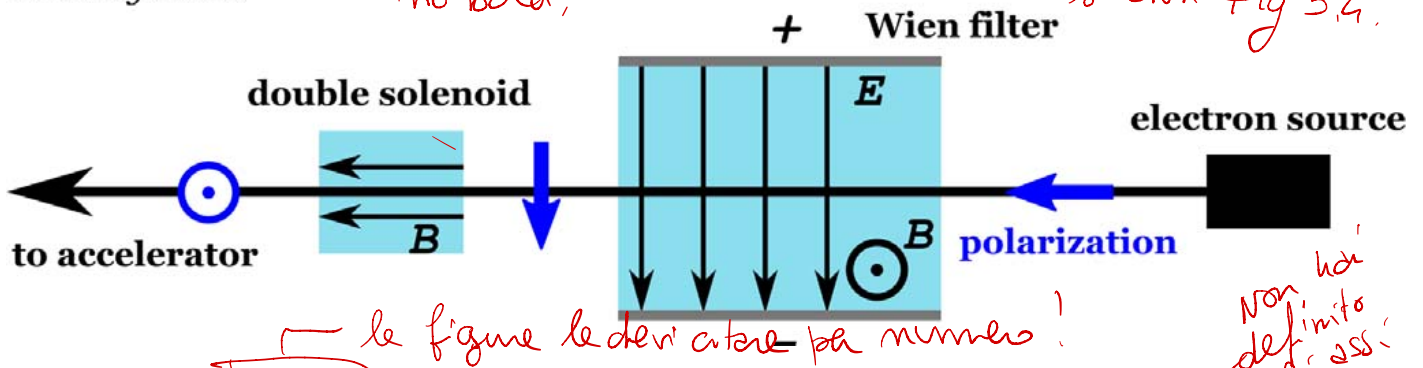


Figure 3.4) Beam line projection. This figure is taken from the paper [16]

Following the picture, the spin of the electrons from the source are rotated first in the XY plane with a 90° rotation, then the subsequent double solenoid align the spin to the vertical direction with another 90° rotation. Once the beam passes the double solenoid, the electrons go through the linac, the microtron and in the end to the experimental hall, where the target of the experiments is installed. During the acceleration stage, the spin follows the precession motion due to the various magnetic fields of the accelerator, the precession, for a relativistic particle, is determined by the BMT equation. However it is not necessary, due to our particular experimental setup, the BMT equation is quite simple: the magnetic field of the various bending magnets that constitute the microtron-cascade are always parallel to the vertical direction, so that the cross product $\vec{B} \times \vec{P} = 0$, and the polarization remain constant. Only the residual horizontal component precedes during the motion. For conventional experiment that involve longitudinal polarization, after the first spin rotation due to Wien filter and the bending magnets close to the electrons source, there is a further rotation to be considered, due to the motion of the particle during the acceleration and recirculation in the microtron. Because of this, the rotation made by the Wien is set in such a way that after the second rotation due to the motion in the accelerator, the polarization has the correct alignment in the experimental hall. The rotation angles of the polarization vector through the accelerator are known from simulations and are also directly measured for relevant energies, for a beam of 570 MeV the rotation angle is 55° with an accuracy of $\pm 2^\circ$. In our case, this further rotation has only a small effect to the residual horizontal component, whose effect is negligible

g sostantivi in italiano si scrivono con le minuscole!
Magnetic → magnetic.

because it is accurately minimized by MAMI operators at the beginning of the beam time. Besides this, the effect of a small horizontal polarization on the asymmetry is small, knowing that typically the transverse asymmetries are one order higher than the PV. At the beginning MAMI was not developed for experiment with transverse polarization, so it's not possible to measure directly the transverse component. However combining the measurement in the XY plane, with the existing setup, it is possible to get the polarization value also in that direction. For this purpose ~~a~~ Moller, Compton and Mott polarimeters are used.

3.2.2 Polarization Measurement

~~Polarization Measurement~~ — queste sono le misure!

To measure the polarization of an electron beam different polarimeters can be used. Here we explain briefly the physics underlying the *Mott polarimeter*, used in the experiment. Consider an electron beam that is sent towards a nucleus of charge Ze . We know from theory [10] that the spin of the incident electron interacts with the electromagnetic field produced by the nucleus. The magnetic field seen by a particle with speed \vec{v} near a nucleus is:

$$\vec{B}_{nucleus} = \frac{-\vec{v} \times \vec{E}_{nucleus}}{c} = \frac{Ze}{mcr^3} \vec{L}$$

This magnetic field is coupled with the magnetic momenta of the electron μ_e .

$$V = -\mu_e \cdot \vec{B}_{nucleus} = \frac{Ze}{mcr^3} \vec{L} \cdot \vec{S}_e \quad (3.4)$$

The second equation represents the spin-orbit interaction potential. This term yields the polarization dependence of the cross section, and it is exploited to obtain the polarization of the incident particles. Indeed the cross section can be modeled highlighting the dependencies on the spin \vec{S} :

$$\sigma(\theta) = I(\theta)[1 + S(\theta) \vec{P} \cdot \vec{n}]$$

Non puoi buttare la
una espiazione senza
spiegare i termini.

Let's consider an incident particle that scatters from a nucleus at an angle θ , as shown in the figure:

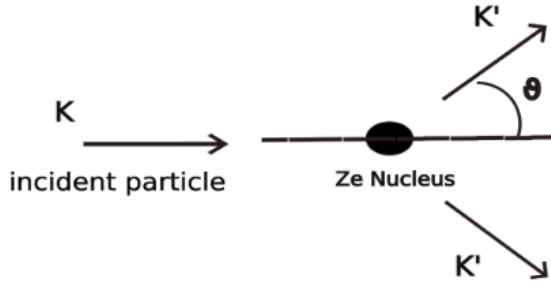


Figure 3.5: Scheme of the Mott scattering, the polarization is orthogonal to the plane, $\vec{n} = \frac{\vec{k} \times \vec{k}'}{|\vec{k} \times \vec{k}'|}$

The direction of \vec{n} depends on whether scattering to the left or right is being considered. Let's suppose our initial beam has a polarization P , and so we compute the asymmetry $A(\theta)$ of the scattered electrons between left (N_L) and right (N_R). N_L and right N_R will be proportional respectively:

$$N_L = N_\downarrow[1 + S(\theta)] + N_\uparrow[1 - S(\theta)]$$

$$N_R = N_\uparrow[1 + S(\theta)] + N_\downarrow[1 - S(\theta)]$$

$$A(\theta) = \frac{N_L - N_R}{N_L + N_R} = \frac{N_\downarrow(1 + S(\theta)) + N_\uparrow(1 - S(\theta)) - N_\uparrow(1 + S(\theta)) + N_\downarrow(1 - S(\theta))}{N_L + N_R} = \dots = P \cdot S(\theta)$$

From the last equation we have a relation which give the beam polarization in terms of $A(\theta)$ (which is what is measured) and the asymmetry function $S(\theta)$ (known also as Sherman function). There are several calculation of the Sherman function, which is well-known for high energy electron scattering.

altrove

The total beam polarization is measured by a Moller polarimeter, in the experimental hall, with the beam polarization oriented longitudinally in the experimental hall. The Moller polarimeter can measure the longitudinal polarization of the beam. The other two polarimeters, Compton and Mott, located behind the injector linear accelerator (ILAC), are sensitive to the longitudinal and the trasverse horizontal components of the beam (with an energy around 3,5 MeV at this stage). The procedure for the alignment is the following: at the beginning of the beam time the Mott polarimeter is used for different settings of the solenoidal field, with the Wien filter angle equal (nominal) to 90° . The aim is to minimize the horizontal polarization component after the rotation performed by the double solenoid, changing the solenoidal magnetic field. Then a second optimization follows, using the Moller polarimeter for different Wien filter angles is performed. With the new Wien filter settings, another measurement is performed with the Mott polarimeter.

3.2.3 Moller and Compton polarimeters

3.3 Experimental Hall Setup

Until now we have described how MAMI produce to accelerate the electrons, however we have not presented the structure where the beam is delivered and various experiments are carried out.

Actually MAMI has 2 different halls, named with the capital letter A followed with a number, which indicate also the different collaboration that work with the experiments. In A2, as an example, photo-nuclear reactions are studied to investigate the fundamental physics at the scale of nuclear dimensions. The experimental hall where the experiment treated described in this thesis is conducted is the A1 hall. We will describe briefly the main operating detectors that are installed and the details that are interesting for the transverse asymmetry measurement.

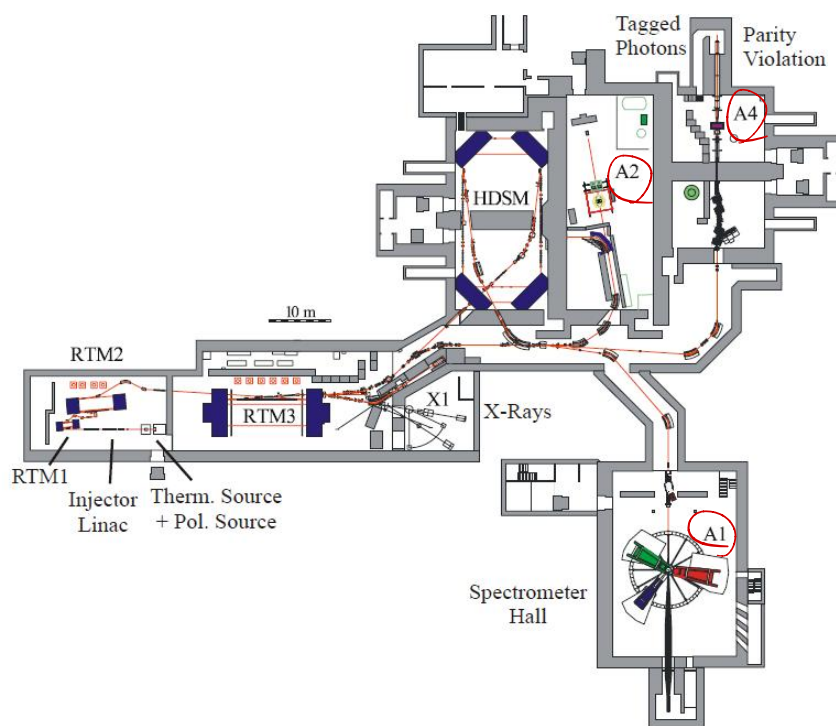


Figure 3.6: Scheme of the accelerator, with the different experimental halls. A third hall previously used for the A4 experiment, measuring the strange quark content of the proton, is now being used for the novel MESA accelerator and its experiments.

In A1, experiment with fixed targets are conducted. The electrons can be delivered with an energy up to 1,6 GeV, after passing the last acceleration stage (HDSM, in the figure). Because the electron energy of our experiment is 570 MeV, the beam will pass through the first acceleration steps, the linac (linear accelerator) and Race-track system and when the desired energy is achieved the electrons will be sent to the A1 experimental hall.

→ Riesci a non spiegarti: Non uscite HDSM e arrivano direttamente da RTM?

In inglese i numeri si scrivono con il punto decimal
non la virgola.

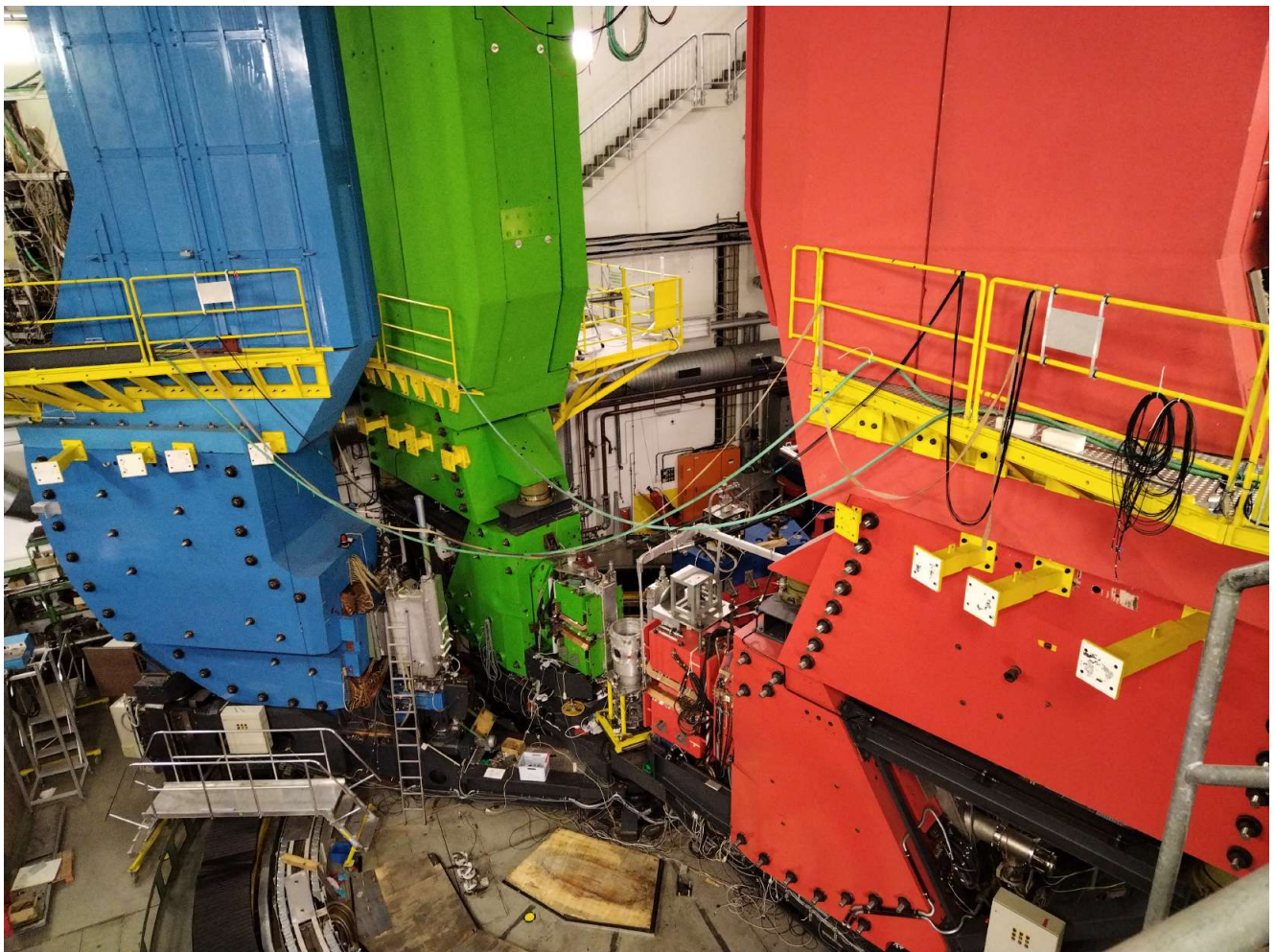


Figure 3.7: Picture of the A1 spectrometers hall, the spectrometers red and blue are used during this experiment. At the center of the picture is possible to observe the scattering chamber.

Inside A1 hall three large magnetic spectrometers are placed on a circular rail-track around the target chamber. These spectrometers were designed and built in 1993 to perform high precision measurement of electron scattering in coincidence with other hadron detection, with a high resolution in the determination of the particle momenta $\frac{\delta p}{p} < 10^{-4}$. The spectrometers develop vertically with a height of 15 m, for this reason the scattered electrons and the other particles are deflected with the use of the magnetic field respect to the scattering plane. The following figure shows the path the particle scattered from the target: The spectrometers used for the transverse asymmetry are the ones shown in the picture. There are multiple reasons why the particle are deflected on the vertical direction; we summarized them in two points.

- reason of space, due to the fact the horizontal setup would not fit with the dimension of the building in addition to the fact that this would not allow to rotate the spectrometers by a variety of angles that the vertical orientation does
- reduce background and noise, in fact the high beam intensity that is possible to reach at MAMI is a source of noise and background event which can be cut off detecting the particle far from the interaction point.

Once a particle is scattered in the acceptance region of the spectrometers, it is deflected by the magnetic field and passes through the drift chamber, which occupies the first third in height of the spectrometers. When the particle is at the height of the platform in the figure 3.8, it impinges on a layer of plastic scintillator, and after that a Cherenkov detector which measures the particle speed v . We have a picture 3.9 of the spectrometers internal, taken during the installation of the two detectors. The determination of both the particle speed v and momenta (drift chamber) allows to identify the particles. Despite the possibilities offered by the already existing setup, for the beam time of interest none of these components was used directly in the estimation of A_n . The reason is due to the high intensity of the beam that is used in the experiment, which is far from

*cercò di limitare l'uso delle
più me persone*

*Principio: tutte le figure si citano con il numero mai "following"
tutte le figure vanno citate da qualche parte.*

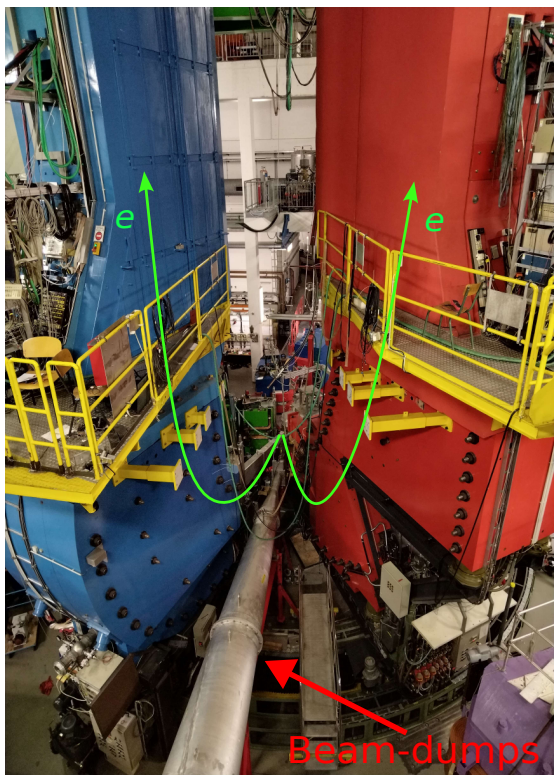


Figure 3.8: Image of the spectrometers of A1 hall. The spectrometers can be rotated using a system of rail-tracks that are visible at the bottom of the image. The electrons are scattered and then deflected in the vertical direction by the magnetic field (green lines). This picture is taken from behind the target. The target is roughly at the center of the image where the two green lines join. The electron are coming from the opposite direction respect with the spectrometers.

with respect to

with ~~to~~

the optimal operating conditions of the components, that are suited for rates lower than the ones expected for beam normal single spin measurements. The spectrometers are used indirectly for the alignment of scattered electrons to the focal plane of our detectors.

Nam mi sembra che ci sia un sistema ottico nei rivelatori che ho usato)

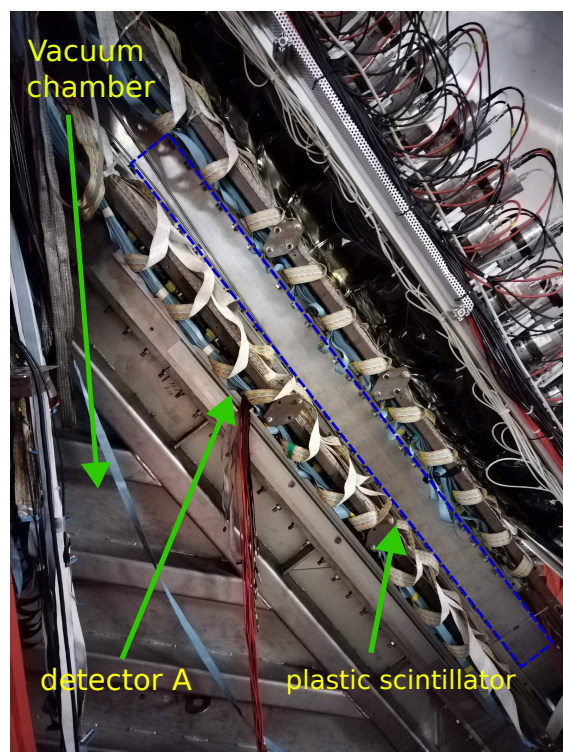


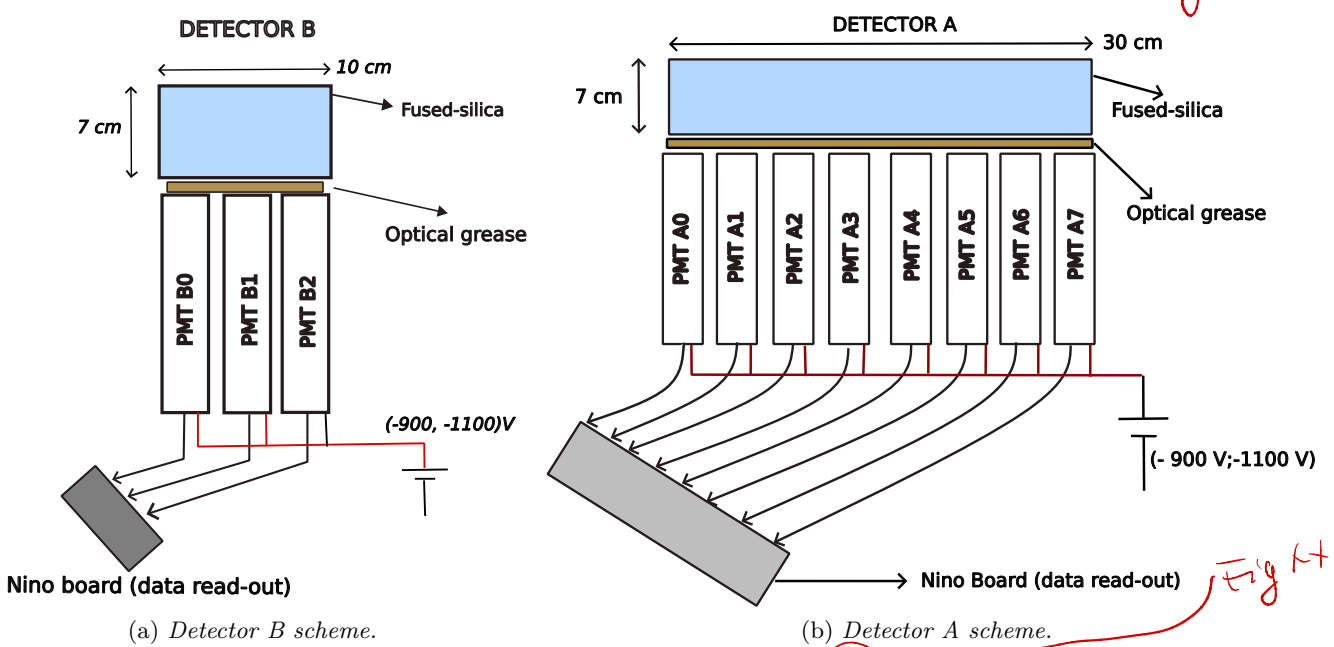
Figure 3.9: Internal of the spectrometer. This image was taken during the installation of the detector A inside the red spectrometer, that is accessible from the platforms visible in the picture 3.8

3.4 Detector Description

Spin ✓

In this section we will describe the electronics and the detectors used to measure the transverse asymmetry. For this experiment we are going to measure the transverse asymmetry at one fixed angle, corresponding to a transferred momentum of $Q = 0.2 \text{ GeV}$. The electrons detection is made via two thin blocks of fused-silica that are coupled to PMTs. When a scattered electron hits the fused-silica (refractive index $n = 1.45$) Cherenkov light is emitted. The emitted Cherenkov light can interact with the electrons of the material, which, in turn, can hit the PMT dynode. This sequence of event triggers the PMT and produce an output signal.

~~will be simplified~~ In the experiment two detectors are installed and read-out independently. The detector A is placed at an angle of $+\theta$, while detector B is placed at $-\theta$. We expect to measure the same absolute value of the transverse asymmetry, with an opposite sign due to the different orientation. The two detector are made by 3 PMTs and 8 PMTs coupled with two blocks of fused-silica, a scheme of the detector ~~(a)~~ is shown below. ~~in Fig. --~~



These two detectors are placed inside the spectrometers presented in , between the top of the drift-chamber, which occupies the first third in height of the spectrometer, and just below a panel of scintillator. During the experiment, the drift chamber of the spectrometers is turn off, and also the PMTs coupled to the spectrometer scintillators are not powered. As we mention above, the scattered electron are deflected in the vertical direction by the magnetic field of the spectrometer. At this moment, it is important to mention the differences between the new and the old electronic setup. In the old electronic setup the output signal of the PMTs was integrated during the time interval of each sub-event, and therefore the single scattered electron could not be counted. The advantage of this method is that the electronics is more simpler. However, this old method is affected by a baseline noise and it is not good for the future experiments with lead target, where the expected rates are lower than the rates on carbon. With the new electronics, all the single electrons are counted, and this will allow the future measurements with lead, improving the accuracy.

Here we report the characteristic of the two detector that are relevant for the data analysis:

- detector B size: $7 \text{ cm} \times 10 \text{ cm} \times 1 \text{ cm}$
- detector A size: $7 \text{ cm} \times 30 \text{ cm} \times 1 \text{ cm}$
- Number of dynodes: 12
- The Power voltage for the PMT in negative, in the range of $(-900 \text{ V}, -1100 \text{ V})$
- refraction index n of the fused-silica is 1.45.

Sarebbe utile dire il funzionamento del PMT, se lo sai.

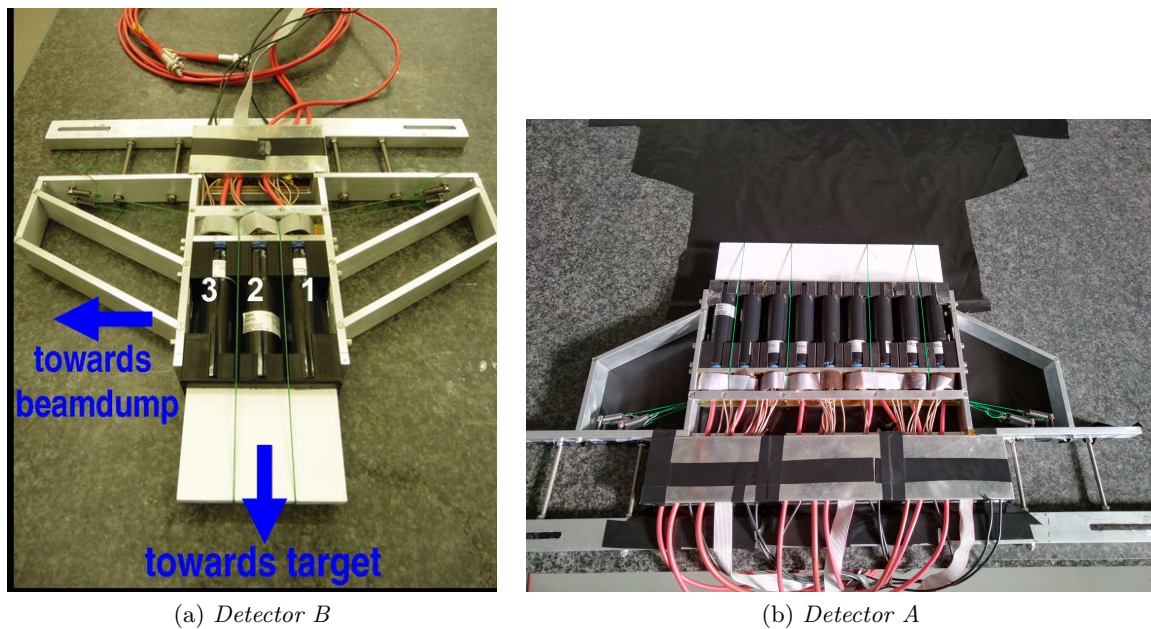


Figure 3.10: Picture of the two detector taken in the clean room. The white blocks are the fused silica that produces the Cherenkov light, the cylinders below are the PMTs.

3.5 Beam Monitors

In MAMI, several monitors are placed along the beam line ~~in order to~~ to check beam quality and measure parameters such as current intensity, energy and relative position of the beam. This section summarizes ~~an explanation of~~ the operating principles of the monitors installed at MAMI. ~~The explanation will be partial, some details will be given in the appendix; however~~ for a complete discussion please refer to the ~~following~~ paper ~~([7])~~. the cose vuoi dire??

The monitors available at MAMI are ~~quite specific for the standard of the particle accelerators~~. Resonant cavities are used to measure the various quantities, with the underlying physical principle that the passage of charged particles through these cavities can excite some electromagnetic resonant modes¹ which can be detected and analyzed by an analog circuit to measure the beam parameters. Before going into the details, it is necessary to define some quantities that will be used later in the explanation. We define r_s the Shunt-impedance discussione as :

$$r_s = \frac{|V_{\parallel}|^2}{P} \quad (3.5)$$

Where P is the power absorbed by the cavity when a particle excites one of the resonant mode, ~~instead~~ V_{\parallel} is defined as the effective voltage ~~surpassed~~ by a charged particle along a straight line, which can be computed as:

change experienced

$$V_{\parallel} = \frac{1}{q} \int_{s_0}^{s^1} \vec{E}_s \vec{e}_s ds \quad \text{cos' } \vec{e}_s ??$$

The Shunt impedance is a measure of the interaction strength between a cavity and a charged particle, and can be expressed ~~also in another way, introducing the Q value of the cavity, W the maximum energy stored and f_r the frequency of resonance;~~ using

$$r_s = \frac{|V_{\parallel}|^2 Q}{2\pi f_r W}$$

¹TM mode, where the magnetic field is completely transverse respect to particle momenta

When the beam travels through the cavity, the particles release energy that excites the mode. The power P_{HF} extracted from the beam is related to the beam current:

$$P = \frac{c}{2\pi\sqrt{\epsilon_r\mu_r}} \left(\frac{x_{m,n}}{R} \right)^2 r_s^2$$

E' lo stesso di ep 3.5? Dose è me iota, perché non uscì?

An antenna is used to decouple part of the energy from the cavity and send it to a circuit which produces an analog output signal. Indicating with κ the coupling constant of the antenna, the previous relation needs to be modified introducing a new factor $\frac{\kappa}{(1+\kappa)^2}$. In a cylindrical resonator, the same type installed at MAMI, the resonance frequency of the different oscillation modes is expressed by the formula

$$f_{m,n,p} = \frac{c}{2\pi\sqrt{\epsilon_r\mu_r}} \sqrt{\left(\frac{x_{m,n}}{R}\right)^2 + \left(\frac{p\pi}{L}\right)^2}$$

The constant in the formula are:

- c is the light speed.
- ϵ_r, μ_r are the magnetic and dielectric costant of the material.
- $x_{m,n}$ it the n-th zero of the m-th Bessel function.
- R and L are the radius of the cylindrical cavity and his lenght.



This formula can be obtained solving the Maxwell equations with cylindrical boundary condition, the eigenvalues are then given by the formula above.

If the frequency of the beam bunch is equal to the resonant frequency $f_{m,n,p}$ of the cavity, a TM mode is excited. At MAMI high quality monitors are installed, quantitatively all the monitors have a $Q \simeq 10000$, that means that $\frac{\nu}{\delta\nu} \simeq 10000$. This means that the frequency of the beam bunch must be very close to the frequency of the resonant cavity. At MAMI the frequency used for all the resonators is 2,449 532 GHz or a multiple of it. The beam bunch frequency is the same, and it is controlled by the MAMI-master oscillation signal, that is the reference signal for all the MAMI monitors.

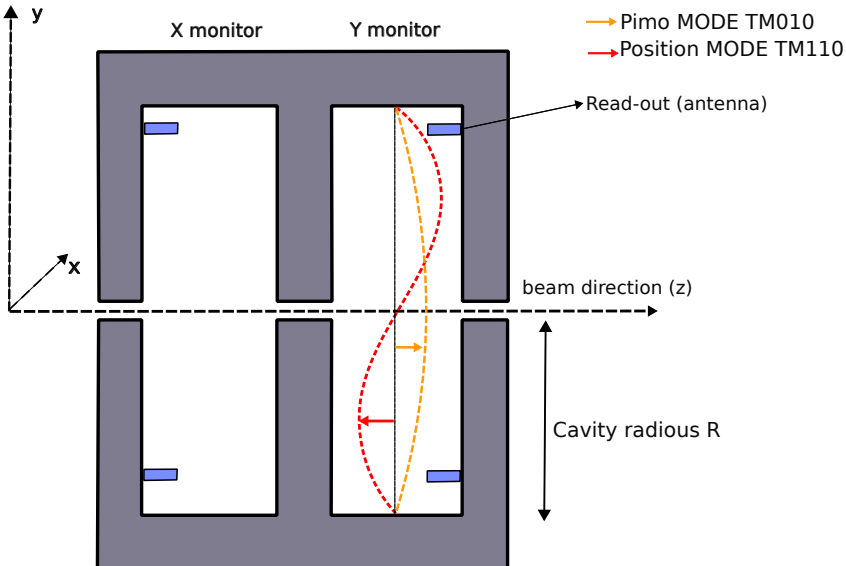


Figure 3.11: Scheme of the Cylindrical cavities installed at MAMI. In red we have the TM_{110} mode, used to measure the position of the beam, in yellow the TM_{010} mode, to measure the intensity of the beam.

Depending on the TM mode excited, we have a different signal in the cavity, so a different signal collected by the antenna. The relevant quantity that is detected is the power P_{HF} absorbed by the antenna. For the TM_{010} mode, the power is

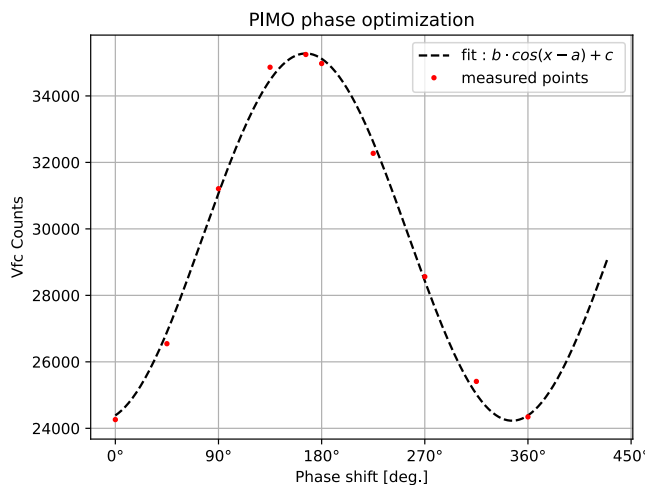
In genere non si separano due fonti principali con le virgolette: o si connettono con qualche predisposizione, oppure si separano con o/;

$$P_{HF} = i^2 r_{010} \frac{\kappa}{(1 + \kappa)^2} \quad (3.6)$$

The power absorbed by the antenna is directly dependent on the beam current. Because the ~~range~~ values are typically in the range of pW to mW, the signal is processed in close proximity of the installed monitors. In the signal process^{*ing*}, the input signal of the antenna is coupled to the master-oscillation signal, so the output signal is given by the formula:

$$U = \sqrt{P_{HF}} \cos(\phi - \phi_{LO}) \quad (3.7)$$

Where the phase ϕ is the phase of the resonant mode or the phase of the beam bunch, while the phase ϕ_{LO} is the phase respect to the master-oscillation signal, and can be adjusted by a phase shifter ~~in~~ of the circuit. The output voltage signal can be read out with the oscilloscope or digitalized and saved with other devices. To measure the beam intensity is important to minimize $\phi - \phi_{LO}$, to maximize the signal amplitude, and then the output signal is ready to be analyzed.



N.B. Le figure devono essere sempre citate nel testo

Figure 3.12: Plot of the phase ϕ versus the output signal. The phase optimization was done selecting the working point in correspondence of the peak.

The measurement of the x, y position follows in principle the same procedure. In this case the TM_{110} is acquired. The reason is clear, because it is possible to calculate that for this mode the r_{shunt} is proportional to the beam position on the x, y plane. So The power absorbed by the antenna can be written:

$$P_{HF} = t^2 r_{110} \frac{\kappa}{(1 + \kappa)^2} K x^2 \quad (3.8)$$

The output signal, that is read by our setup, is proportional to the square root of the absorbed power:

$$\sqrt{\cancel{(P_{HF})}} = costant \cdot U \cdot i \cdot x \quad (3.9)$$

The beam parameter are then given inverting the above formula

$$x \simeq \frac{\sqrt{(P_{HF})}}{i} \quad (3.10)$$

Where the exact conversion coefficients are not known, and are determined during the calibration phase, at the beginning of the beam time. To measure the beam energy, a different approach is used. In principle, the energy monitor (ENMO) consist of 2 cavities in the RTM3. One is located in the last recirculation pipe, the other one on the part of the beam line, where the acceleration takes place. The two monitors are synchronized to the master oscillation and measure the phase of the bunches of electrons. When during their travel from the first cavity to the second cavity, the beam passes through the magnet and does one half turn. Now, if the energy is slightly higher, the radius of the turn will be slightly longer. This means that there is an extra time between the two bunches, that can be measured as a small phase shift in the 570 MeV recirculation. From this it is possible to obtain a value for the difference of energy to the nominal energy.

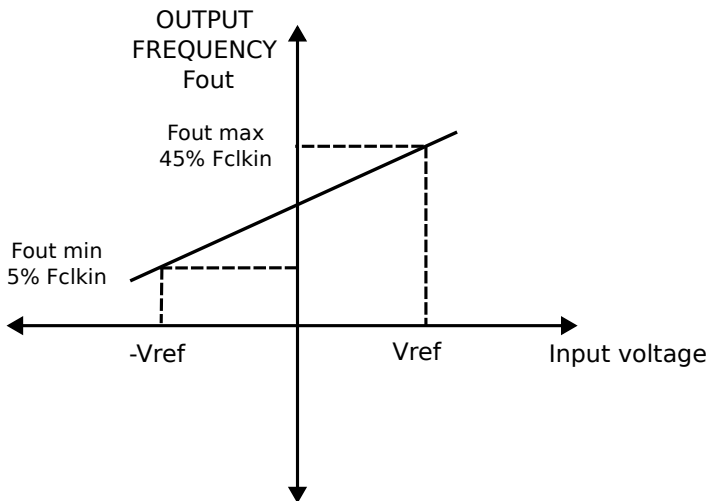
3.5.1 Beam stabilization

The beam stabilization is an essential component of the experiment. The values of A_n that we want to measure are in the order of ten *ppm*, so it is important to reduce other contributions that can be related to variations in the beam parameters.

3.6 Electronics

3.6.1 VFCs Voltage to Frequency Converters

Some parameters which describe the beam are needed in order to take into account possible effects in the measurement of the transverse asymmetry. The relevant data are the position in the (x, y) plane, the incident angles on the target, the current and energy of the beam. All this values are collected using the already existing monitors. To collect the data from the monitors, single and multichannel, synchronous voltage-to-frequency converters (AD7742) are used. These devices contain an analog modulator that is able to convert the input voltage into an output pulse train, whose frequency is proportional to the input voltage.



The VFCs are powered with an external voltage of 5 V. They measure an input voltage in the range of $(-V_{ref}, V_{ref})$. An external clock signal, with a frequency $F_{CLKIN} = 5.88$ MHz is created externally and synchronous to the gate-length. The analog input signal is sampled with by a switched capacitor, with a rate that is equal to F_{CLKIN} . The comparator produces a number pulses; the frequency of the output signal is proportional to the input voltage, with $-V_{ref}$ equal to $0.5\% \cdot f_{CLKIN}$ and $+V_{ref}$ equal to $0.45\% \cdot f_{CLKIN}$ [1], where the first correspond to 0.0 V in input and the second to V_{ref} . The relation between the output frequency and the input voltage is the following:

Figure 3.13: Frequency versus Voltage

$$V_{in} = V_{ref} \left(2 \frac{f_{out} - 5\% F_{CLKIN}}{40\% \cdot F_{CLKIN}} - 1 \right) \quad (3.11)$$

The data are acquired counting the number of pulses that come from the comparator, so we can substitute to f the number of pulses (the two quantities are proportional), and we end with:

$$V_{in} = V_{ref} \left[2 \cdot \frac{N_{\text{pulses}} - 5\% N_{CLKIN}}{40\% N_{CLKIN}} - 1 \right] \quad (3.12)$$

3.6.2 Nino Board

The NINO board is our data acquisition system for the PMT counts. It is made by 32 analog input channels and it is powered with ± 5 V. Each channel has an attenuator, and the signal passes through that before going to the Comparator, which compares the signal to the threshold. The Output signal is a low-voltage differential signal (LVDS). Each comparator can handle eight channels and for each of them it is possible to define a global threshold. With the current settings of NINO board, it is possible to change the threshold of each channel acting on another value, the attenuation, which decreases the value of the global threshold. Attenuation and threshold are set using 12 bit DACs, corresponding to interval of (0; 4095). The NINO board is designed in

such a way that collects the input charge of the signal, operating with a 30 pF capacitor. The output signal amplitude is proportional to the input charge, and it is sent to the discriminator. Our interest is only to count the number of scattered electron, so we do not intend to measure the input charge, but only a signal is produced or not.

Two Nino board are used in the experiment, one for detector A and one for detector B. For the experiment discussed in this thesis, we will use only 8 channel for detector A and 3 channel for detector B, since this is the

Non serve una reazione a parte,
a meno che tu non intenda svincolare.
Forse queste reazioni non
servono se non ci hai lavorato
direttamente

concluso



Figure 3.14: Nino Board

number of the input signals coming from the two detectors. For the future experiments more channel will be used, splitting the analog input signal in 4 different signal, sending it to 4 different input channel of the board. This is useful because changing individually the attenuation value, we can define 4 different thresholds for the same signal coming from a single PMT. ~~This is useful to compare different values of threshold, for example to study how the noise affects the measurement, and see what is the right compromise between signal and noise ratio.~~ The way we selected the threshold is explained in the following chapter (Analysis).
 mm bln

3.6.3 Master Board

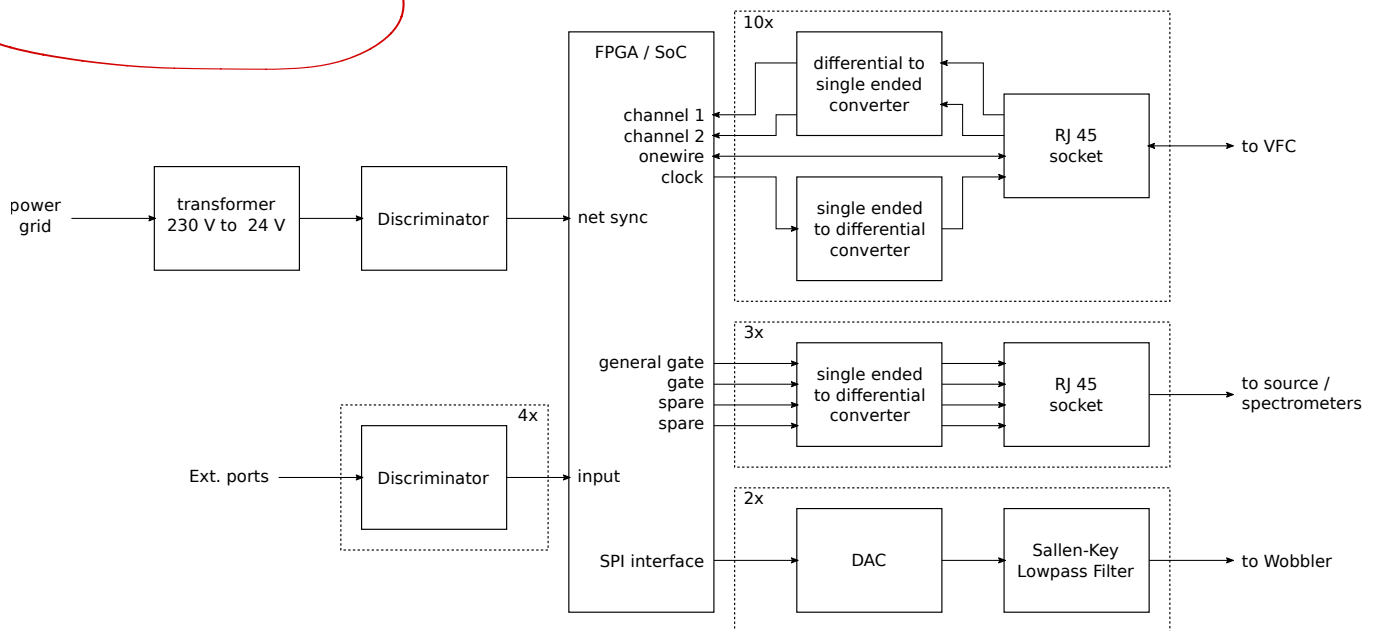


Figure 3.15: Scheme of the master-board, the device that coordinates all the electronics for the experiments, and send the data to the computer in the control room.

manca testo